

# Modeling Parabolic Pulse Formation in Mode-Locked Laser Cavities

Brandon G. Bale<sup>\*</sup> and J. Nathan Kutz<sup>†</sup>

*Abstract*—Self-similarity is a ubiquitous concept in the physical sciences used to explain a wide range of spatial- or temporal-structures observed in a broad range of applications and natural phenomena. Indeed, they have been predicted or observed in the context of Raman scattering, spatial soliton fractals, propagation in the normal dispersion regime with strong nonlinearity, optical amplifiers, and mode-locked lasers. These self-similar structures are typically long-time transients formed by the interplay, often nonlinear, of the underlying dominant physical effects in the system. A theoretical model shows that in the context of the universal Ginzburg-Landau equation with rapidly-varying, mean-zero dispersion, stable and attracting self-similar pulses are formed with parabolic profiles: the zero-dispersion similariton. The zero-dispersion similariton is the final solution state of the system, not a long-time, intermediate asymptotic behavior. An averaging analysis shows the self-similarity to be governed by a nonlinear diffusion equation with a rapidly-varying, mean-zero diffusion coefficient. Indeed, the leading-order behavior is shown to be governed by the porous media (nonlinear diffusion) equation whose solution is the well-known Barenblatt similarity solution which has a parabolic, self-similar profile. The alternating sign of the diffusion coefficient, which is driven by the dispersion fluctuations, is critical to supporting the zero-dispersion similariton which is, to leading-order, of the Barenblatt form. This is the first analytic model proposing a mechanism for generating physically realizable temporal parabolic pulses in the Ginzburg-Landau model. Although the results are of restricted analytic validity, the findings are suggestive of the underlying physical mechanism responsible for parabolic (self-similar) pulse formation in lightwave transmission and observed in mode-locked lasers.

*Keywords:* Mode-locked lasers, Similaritons, Self-similarity, Dispersion-management

## 1 Introduction

Self-similarity is a ubiquitous phenomena exhibited in a broad range of physical and biological systems [4]. It is particularly prevalent in nonlinear dissipative systems where initial transients are attenuated and the solution approaches a self-similar form at long times, i.e. the intermediate asymptotic regime [4]. In this manuscript, we show that a rapidly-varying, mean-zero dispersion fluctuation in the Ginzburg-Landau equation results in the spontaneous formation of breathing, self-similar parabolic structures (Barenblatt solutions). This attracting state, from a Poincaré map point of view, is the steady-state of the system and not a transient, intermediate pulse form typical of self-similarity solutions. Such solutions have been recently observed experimentally [12] and touched upon theoretically [3] in the context of a mode-locked laser. However, the previous theory fails to capture the detailed pulse shape, its attracting nature, and its broader applicability. Here, we provide the first theoretical description of such an *attracting state* which arises in the context of the Ginzburg-Landau model with rapidly-varying, mean-zero dispersion. The breathing parabolic nature of the solution is driven by the mean-zero dispersion fluctuations while the attracting behavior arises from the dissipative terms in the GL equation. Thus the self-similar parabolic structures result as a novel hybrid of dispersion-management techniques and dissipative self-similarity.

The existence of self-similarity implies a certain spatial and/or temporal order in the system that can not only be used to gain insight into the inter-dependences of a given system, but can often be exploited from an analytic point of view. The simplest example of self-similar behavior arises from considering the heat equation, which is the prototypical model for introducing the concept of self-similarity and its transient, long-time behavior [7]. Certain nonlinear generalizations of the heat equation, i.e. the porous media equation, have also been considered and their self-similar behavior (Barenblatt solutions) assessed [14]. Much of the extensive interest in the porous media equation arises from nonlinear diffusive phenomenon in thermal waves [20], flow of thin films [19], groundwater flow [5], population dynamics [16], dispersion-managed systems [6] and mode-locked lasers [3]. The mathematical analysis of the porous me-

<sup>\*</sup>B. Bale is with the Photonics Research Group, Aston University, Birmingham UK B4 7ET

<sup>†</sup>J. N. Kutz acknowledges support from the National Science Foundation (DMS-0092682). J. N. Kutz is with the Department of Applied Mathematics, University of Washington, Box 352420, Seattle, WA 98195-2420.

dia equation suggests that unlike its linear counterpart, its solutions have compact support and finite speeds of propagation. In contrast to these diffusive processes, self-similarity has also been exhibited as the long-time transient in certain amplifier systems [2, 8]. The term “similariton” commonly implies the combination of some underlying self-similar structure with soliton-like (dissipative soliton) persistence of a localized solution. This use of the term “similariton” in the context of mode-locked lasers has been widely used and is also observed in a broad range of other applications.

A perturbed version of the porous media equation arises in the dynamics of the GL equation with a rapidly-varying, mean-zero dispersion. The resulting self-similar, parabolic structure results directly from the dispersion fluctuations. The importance of dispersion-management (DM) and its impact on physical systems is well known. DM solitons are critical for characterizing dispersion managed systems which arise, for instance, in optical fiber communication systems [10, 11, 18] and Bose-Einstein condensates (BECs) [13, 17]. These solutions arise in a Hamiltonian system context and have a Gaussian form. Thus they are not attractors to the underlying system. In contrast, more general Ginzburg-Landau models include dissipative effects that modify the behavior so that attracting states are possible. It is these dissipative terms that render the parabolic breathers an attractor. Such an example arises in mode-locked lasers [3, 12] and BECs [15]. Thus the periodic, mean-zero dispersion fluctuations with dissipative effects are critical for supporting the attracting parabolic states.

## 2 Governing Equations

The cubic-quintic Ginzburg-Landau (GL) equation

$$iu_t + \frac{1}{2}d(t)u_{xx} + |u|^2u = i\delta u + i\beta|u|^2u + i\alpha u_{xx} - i\sigma|u|^4u \quad (1)$$

describes a variety of nonequilibrium phenomena (See [19] and references therein). In the context of mode-locked lasers,  $t$  is the propagation distance that the pulse travels in a laser cavity,  $x$  is the retarded time,  $u$  is the complex envelope of the electric field,  $d$  is the group velocity dispersion coefficient,  $\delta$  is the linear gain-loss coefficient,  $i\alpha u_{xx}$  accounts for spectral filtering ( $\alpha > 0$ ),  $\beta|u|^2u$  represents the nonlinear gain which arises from saturable absorption ( $\beta > 0$ ), and  $\sigma (> 0)$  is the saturation of the nonlinear gain.

Here,  $d(t)$  characterizes the given dispersion fluctuations (map) in the system. If the right-hand side of (1) is perturbatively small, the leading-order equation is the well-known nonlinear Schrödinger equation (NLS) whose soliton solution ( $d > 0$ ) results from a fundamental balance between linear dispersion and cubic nonlinearity. The evolution of the laser cavity dynamics governed by (1) is demonstrated in Fig. 1.

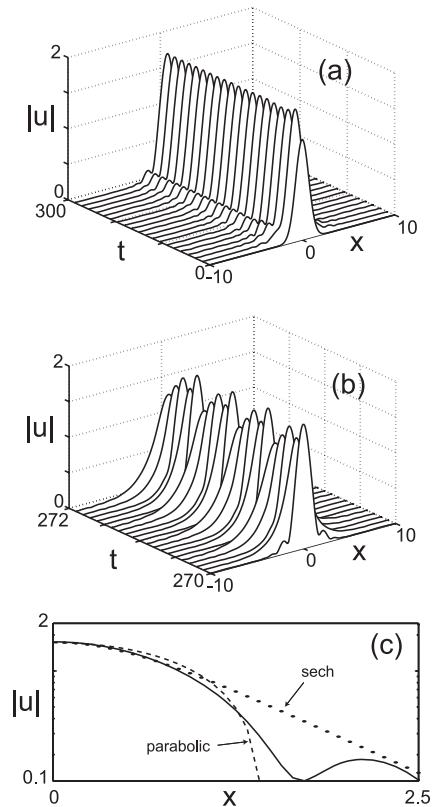


Figure 1: Attracting dynamics of the solution (a) and its breathing dynamics (b) obtained from numerical simulation of the GL equation (1) from a Gaussian initial condition with  $\delta = \alpha = 0$ ,  $\beta = \sigma = 0.1$ , and  $\epsilon = 0.5$ . (a) The output is shown at the beginning of each dispersion map while (b) shows the last four intra-period fluctuations. (c) Comparison of the numerical solution (solid) with a quadratic Barenblatt profile (dashed) and hyperbolic secant pulse (dots). The tail structure is exhibited in experiments [12].

In this manuscript, we investigate (1) when the dispersion length  $T$  is much longer than the typical period  $P$  of the dispersion map, so that

$$\epsilon = P/T \ll 1 \quad (2)$$

and the dispersion fluctuations occur on a rapid scale. The period  $P$  is simply determined by the physical length of the laser cavity while the dispersion length  $T$  is related to the pulse width of the mode-locked pulses. Specifically, the dispersion length is the length it takes for the full-width, half-maximum pulse width to double in the absence of nonlinearities [1]. For convenience and simplicity, we let

$$d = d(t/\epsilon) = \cos(2\pi t/\epsilon). \quad (3)$$

Note that although the results apply to a general  $d(t)$ , it will prove helpful to consider the particular case here of a simple sinusoidal dispersion map.

Simulations suggest that the dispersion fluctuations must occur on a rapid-scale in order for the parabolic states to persist. Such a clear scale separation between the dispersion map period and the fundamental dispersion and nonlinearity scale suggests the application of a multi-scale transformation technique. The transformation procedure considered relies on the Green's function of the linear part of the left hand side of (1) since it accounts explicitly for the dispersion fluctuations. Using Fourier transforms, it is easy to calculate that the Green's function for the linear Schrödinger equation [6]

$$i \mathbf{G}_t + \frac{1}{2} d(t/\epsilon) \mathbf{G}_{xx} = 0, \quad (4)$$

with  $\mathbf{G}(x, x', 0) = \delta(x - x')$  is given by

$$\mathbf{G}(x, x', t) = \frac{\exp(i\pi/4)}{\sqrt{4\pi\mu(t)}} \exp\left(\frac{-i(x - x')^2}{4\mu(t)}\right). \quad (5)$$

Here  $2\mu(t) = \int_0^t d(s)ds \sim O(\epsilon)$  is the accumulated dispersion for a rapidly-varying, mean-zero map.

The transformation is performed by introducing the new function  $A(x, t)$  defined by

$$A(x, t) = \int \mathbf{G}^\dagger(x, x', t) u(x', t) dx'. \quad (6)$$

The evolution equation for  $A$  can be found by using the adjoint relation  $u(x, t) = \int \mathbf{G}(\xi, x, t) A(\xi, t) d\xi$ . Plugging this into the governing equation (1), making use of (4), then multiplying by the adjoint  $\mathbf{G}^\dagger(\xi, x, t)$  and integrating with respect to  $\xi$  gives an exact transformation. At this point no approximations have been made—the transformation from  $u$  to  $A$  is simply a linear change of variables. Since  $\mu \sim \epsilon \ll 1$ , the integrals can be approximated using stationary-phase asymptotics [6]. Expanding the integrals about the stationary phase points gives an approximate evolution for  $A$  where  $q_i$  can be any of the small parameters  $\delta, \alpha, \mu, \beta$ , or  $\sigma$ . This gives the effective evolution for  $A(x, t)$  that neglects higher order terms since the equation parameters  $\delta, \alpha, \beta$ , and  $\sigma$  are small and  $\mu \sim \epsilon \ll 1$ .

The effective equation can be put into a more transparent form with the amplitude-phase decomposition

$$A(x, t) = \sqrt{\rho(x, t)} \exp(i\Theta(x, t)). \quad (7)$$

Inserting (7) into the equation for  $A(x, t)$  yields

$$\rho_t = \mu(t)(\rho^2)_{xx} - 2\rho(\delta - \beta\rho + \sigma\rho^2) + \alpha\left(\rho_{xx} - \frac{\rho_x^2}{2\rho} - 2\rho\Theta_x^2\right) \quad (8a)$$

$$\Theta_t = -\rho - 2\mu(t)\rho\Theta_{xx} + \alpha\left(\Theta_{xx} + \frac{1}{\rho}\rho_x\Theta_x\right). \quad (8b)$$

A key observation is for  $\mu > 0$  the phase equation (8b) is ill-posed whereas for  $\mu < 0$  the amplitude equation (8a) is ill-posed. This problem is an artifact of the averaging

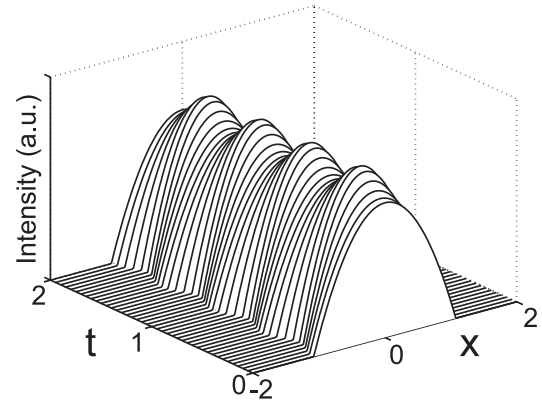


Figure 2: Typical evolution of the Barenblatt similarity solution (10) over four dispersion map periods with  $D(t) = \cos(2\pi t/\epsilon)$ . The breathing dynamics is induced by the periodically varying diffusion coefficient  $\mu(t) \sim O(\epsilon)$ .

process and can be treated via regularization or by including higher order correction terms [6]. In contrast to other averaging techniques used on dispersion managed systems [9], we emphasize that the averaging technique used here retains the critical dependence of the parameter  $\mu$  on  $t$ . This plays a key role in the stabilization of the parabolic state. Indeed, if the  $\mu(t)$  parameter is averaged out to be a constant, the theory fails to correctly capture the breathing nature of the solutions. Specifically, the profile undergoes typical self-similar broadening until the expansion formally breaks down at  $t \sim 1/\sqrt{\epsilon}$  [6].

### 3 leading order barenblatt self-similarity

In the limit where the dissipative perturbations on the right hand side of (1) are small in comparison with the dispersion map, i.e.  $(\delta, \beta, \sigma, \alpha) \ll \epsilon < 1$ , the leading order amplitude equation is governed by the porous media equation [3]

$$\rho_t = \mu(t)(\rho^2)_{xx}. \quad (9)$$

The porous media equation has the Barenblatt similarity solution [4]

$$|u|^2 \approx \rho(x, t) \sim \frac{1}{12(\gamma+t_*)^{1/3}} \left[ a_*^2 - \left( \frac{(x-x_*)}{(\gamma+t_*)^{1/3}} \right)^2 \right]_+ \quad (10)$$

where  $\gamma = \gamma(t) = 2 \int_0^t \mu(s)ds$ ,  $f_+ = \max(f, 0)$  and the solution is characterized by the three parameters  $(a_*, t_*, z_*)$  which represent the mass, center position, and pulse-width of the solution respectively. Note that  $u \approx A$  when  $\epsilon \ll 1$  [6]. Here, to first order in  $\mu \sim \epsilon$ , the evolution equation for the amplitude decouples from the equation for the phase. Figure 2 illustrates the typical time-dependent evolution of the Barenblatt solution (10) over

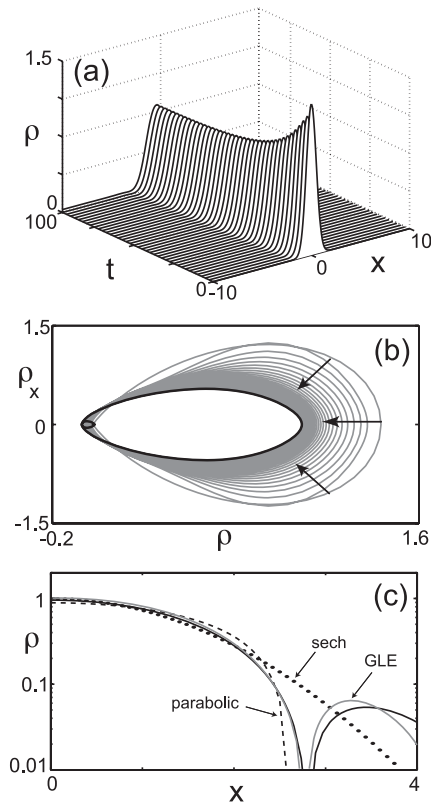


Figure 3: Attracting dynamics of the solution (a) and its phase-plane (b) obtained from numerical simulation of the amplitude equation (11) from a Gaussian initial condition with  $\delta = 0$ ,  $\beta = \sigma = 0.1$ , and  $\epsilon = 0.5$ . The output is shown at the beginning of each dispersion map. (c) Comparison of the parabolic solution from solving (11) numerically (solid black) with the solution from the full governing Ginzburg-Landau equation (1) (solid grey), a quadratic Barenblatt profile (dashed) and hyperbolic secant pulse (dots). The tail structure is also exhibited in experiments [12].

four cavity round trips. We emphasize that the breathing dynamics results from the periodic fluctuations in the integral of the cumulative dispersion  $\gamma(t)$ . Indeed, the averaging technique used here retains the oscillatory nature of the dispersion map in the form of a  $t$ -dependent oscillatory coefficient in Eqs. (10). This oscillatory variation suppresses the structure from undergoing its usual self-similar broadening and allows for stable self-similar breathers.

#### 4 Evolution Dynamics

Although the Barenblatt solution (10) captures the fundamental self-similar structure, it is not the attracting state of the underlying system. This is expected since we have neglected the dissipative terms needed to cre-

ate an attractor. Further, the Barenblatt solution has unphysical discontinuous derivatives at its edges. So although insightful, it is a mathematical idealization that is physically unrealizable. In many applications, spectral filtering is much weaker than other dissipative terms, i.e.  $\alpha \ll (\delta, \beta, \sigma, \mu)$ . In this case, the amplitude equation

$$\rho_t = \mu(t)(\rho^2)_{xx} - 2\rho(\delta - \beta\rho + \sigma\rho^2), \quad (11)$$

is still decoupled from the phase equation. Although exact solutions to (11) are not attainable, this equation sheds light as to why parabolic states persist in this system. Specifically, for small values of the parameters  $\delta$ ,  $\beta$  and  $\sigma$ , equation (11) is perturbatively close to (9). Likewise, the solutions of the two equations should also be perturbatively close so that the leading order behavior of (11) inherits the self-similar Barenblatt structure of (10). Note that this implies that (11) is not strictly self-similar as certain symmetries associated with (9) are broken. Regardless, the inclusion of dissipative terms allows for an attracting parabolic breathers to exist for a wide range of parameter space. Further, numerical simulations suggest the parabolic states are robust to a variety of perturbations including white-noise fluctuations.

Figure 3 shows the numerical simulation of (11) from initial amplitude  $\rho(x, 0) = \sqrt{2}\exp[-x^2]$ . The output point in the Poincaré map is taken to be at the beginning of each map period. Figure 3(a) shows that the initial Gaussian structure quickly settles to a steady state solution in the Poincaré map. In contrast to the Barenblatt solution, the output pulse profile here has finite derivatives at its edges. Figure 3(b) plots the corresponding  $(\rho, \rho_x)$  phase plane and shows that there is indeed an attracting homoclinic orbit (solid line) which represents the steady state solution. To show that this attracting state has a parabolic profile, the output pulse (once settled to the parabolic breather), along with a Barenblatt quadratic (dashed) and hyperbolic secant (dotted) fit is plotted in Fig. 3(c). In addition, the numerical solution for the Ginzburg-Landau equation (1) with parameters  $\alpha = \delta = 0$ ,  $\beta = \sigma = 0.1$ , and  $\epsilon = 0.5$  is included (solid grey). This shows that the solutions to (1) and (11) are perturbatively close as expected. Further, the remarkable agreement between the solution profile of (11) agrees with experiments [12]. Unlike the Barenblatt solution, the parabolic solution to (11) is a physically realizable, smooth profile that correctly captures the tail structure and attracting nature observed in experiments [12].

Similar to dispersion-managed solitons [10, 11, 18] where the dispersion map induces Gaussian-like breathing solutions, the periodic variation of  $\mu(t)$  allows for the parabolic solution to breath within each period. Figure 4(a) shows the pulse evolution (once settled to the parabolic breather) over two periods. Here we see the varying coefficient  $\mu$  in (11) forces both broadening and compression. Indeed, the oscillatory variation suppresses

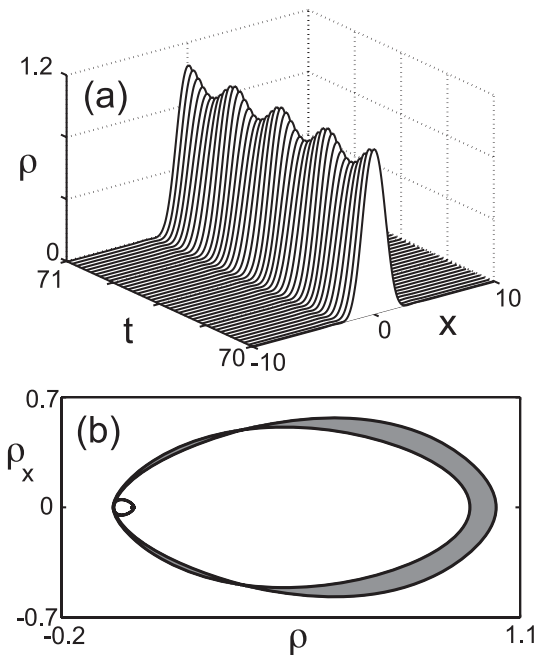


Figure 4: Intra-cavity solution (a) and phase plane (b) obtained from numerical simulation of the amplitude equation (11) once settled to its stable breathing state with parameters  $\delta = 0$ ,  $\beta = \sigma = 0.1$ , and  $\epsilon = 0.5$ . The output is shown over two dispersion map periods. The restricted space for allowed homoclinic orbits in the phase plane (gray area) shows that the dispersion map allows for parabolic pulse propagation.

the parabolic structure from undergoing its usual broadening. This allows for stable self-similar propagation. Figure 4(b) illustrates the phase-space dynamics in the  $(\rho, \rho_x)$  plane corresponding to the breathing parabolic profiles over one period. In essence the rapidly varying periodic dispersion map restricts the space of the allowed homoclinic orbits, thus resulting in ZD similarity propagation. It should also be noted that during the intra-period evolution, the pulse becomes more hyperbolic secant-like during certain portions of the cavity period. This is similar to dispersion-managed solitons for which the pulse is Gaussian at the period points, but more hyperbolic secant-like during certain points of the dispersion map [10, 11, 18].

## 5 Conclusion

In conclusion, we have shown that the underlying behavior in the Ginzburg-Landau equation with rapidly-varying, mean-zero dispersion results in a perturbed version of the nonlinear (porous media) diffusion equation with mean-zero diffusion coefficient. The dispersion fluctuations are directly responsible for generating the mean-

zero diffusion coefficient which allows the solution to be a steady-state solution (from a Poincaré map point of view) as opposed to the standard, long-time self-similar behavior that is only an intermediate state. The dissipative contributions in the GL equation make the parabolic structure an attracting state of the system. Thus the two driving mechanisms of parabolic propagation are the mean-zero dispersion map which generates self-similarity (to first order), and dissipation which makes the self-similar structure an attractor. The combination of the two phenomena result in the formation of the parabolic breathers that have been recently observed experimentally in the context of mode-locked lasers [12]. The theory produces the governing evolution equation (11) that has solutions that agree well with experiment down to the observed oscillatory tail structure.

## References

- [1] G.P. Agrawal. *Nonlinear Fiber Optics*. Academic Press, 1995.
- [2] D. Anderson, M. Desaix, M. Karlsson, M. Lisak, and M. L. Quiroga-Teixeiro. *J. Opt. Soc. Am. B*, 10:1185, 1993.
- [3] B. G. Bale, J. N. Kutz, and F. Wise. *Opt. Lett.*, 33:911, 2008.
- [4] G.I. Barenblatt. *Scaling, Self-similarity, and Intermediate Asymptotics*. Cambridge, 1996.
- [5] J. Bear. *Dynamics of Fluid in Porous Media*. Elsevier, 1972.
- [6] J. Bronski and J.N. Kutz. *Physica D*, 108:315, 1997.
- [7] L.C. Evans. *Partial Differential Equations*. American Mathematical Society, 1998.
- [8] M. Fermann, V. Kruglov, B. Thomsen, J. Dudley, and J. Harvey. *Phys. Rev. Lett.*, 84:6010, 2000.
- [9] I. Gabitov, T. Schafer, and S. K. Turitsyn. *Phys. Lett. A*, 265:274, 2000.
- [10] I. R. Gabitov and S. K. Turitsyn. *Opt. Lett.*, 21:327, 1996.
- [11] J. P. Gordon and L. F. Mollenauer. *Opt. Lett.*, 24:223, 1999.
- [12] F. Ilday, J. Buckley, W. Clark, and F. Wise. *Phys. Rev. Lett.*, 92:213902, 2004.
- [13] S. Inouye, M. R. Andrews, J. Stenger, H.-J. Miesner, D. M. Stamper-Kurn, and W. Ketterle. *Nature*, 392:151, 1998.
- [14] S. Kamin. *Asymptotic behavior of solutions of the porous media equation with absorption in Nonlinear Diffusion Equations and Their Equilibrium States*. J. S. W. M. Ni and L. A. Peletier, Springer, 1988.

- [15] J. N. Kutz. *Physica D*, page doi:10.1016/j.physd.2008.07.017, 2009.
- [16] J. D. Murray. *Mathematical Biology*. Springer, 1990.
- [17] J. L. Roberts, N. R. Claussen, Jr. James P. Burke, Chris H. Greene, E. A. Cornell, and C. E. Wieman. *Phys. Rev. Lett.*, 81:5109, 1998.
- [18] N. J. Smith, F. M. Knox, N. J. Doran, K. J. Blow, and I. Bennion. *Elec. Lett.*, 32:54, 1996.
- [19] T. P. Witelski. *IMA J. Appl. Math.*, 54:227, 1995.
- [20] Y. B. Zeldovich and Y. P. Raizer. *Physics of Shock Waves and High-Temperature Hydrodynamics Phenomena*. Academic Press, 1967.